AD_____

Award Number: W81XWH-06-1-0732

TITLE: Temporal Subtraction of Digital Breast Tomosynthesis Images for Improved Mass Detection

PRINCIPAL INVESTIGATOR: Christina M. Li
James T. Dobbins, III, Ph.D.

CONTRACTING ORGANIZATION: Duke University
Durham, NC 27708

REPORT DATE: October 2007

TYPE OF REPORT: Annual Summary

PREPARED FOR: U.S. Army Medical Research and Materiel Command
Fort Detrick, Maryland 21702-5012

REPORT DOCUMENTATION PAGE

Form Approved
OMB No. 0704-0188

1. REPORT DATE	2. REPORT TYPE	3. DATES COVERED
01-10-2007	Annual Summary	15 Sep 2006 – 14 Sep 2007

4. TITLE AND SUBTITLE

Temporal Subtraction of Digital Breast Tomosynthesis Images for Improved Mass Detection

5a. CONTRACT NUMBER

5b. GRANT NUMBER
W81XWH-06-1-0732

5c. PROGRAM ELEMENT NUMBER

6. AUTHOR(S)

Christina M. Li
James T. Dobbins, III, Ph.D.

Email: christina.li@duke.edu

5d. PROJECT NUMBER

5e. TASK NUMBER

5f. WORK UNIT NUMBER

7. PERFORMING ORGANIZATION NAME(S) AND ADDRESS(ES)

Duke University
Durham, NC 27708

8. PERFORMING ORGANIZATION REPORT NUMBER

9. SPONSORING / MONITORING AGENCY NAME(S) AND ADDRESS(ES)
U.S. Army Medical Research and Materiel Command
Fort Detrick, Maryland 21702-5012

10. SPONSOR/MONITOR'S ACRONYM(S)

11. SPONSOR/MONITOR'S REPORT NUMBER(S)

12. DISTRIBUTION / AVAILABILITY STATEMENT
Approved for Public Release; Distribution Unlimited

13. SUPPLEMENTARY NOTES

14. ABSTRACT
Digital breast tomosynthesis (DBT) strives to overcome the obstacles presented in conventional 2D mammography by taking multiple projections over a fixed angle and reconstructing volumetric data isolates overlying anatomy from in-plane structures and amplify the conspicuity of lesions. Temporal subtraction automates the process of comparative analysis by using two images taken sequentially and subtracting them in order to find temporal discrepancies. The purpose of this project is to determine the feasibility of using temporal subtraction on DBT phantom images to allow for easier and earlier detection of breast cancer than with either technique alone. The investigator acquired initial tomosynthesis images with the compressible and deformable breast phantom using materials to simulate the breast parenchyma. This was a first step to see if the physical breast phantom originally conceived in theory would work in practice. Unfortunately, the materials used for the breast tissues did not provide a realistic enough breast simulation. Further work must be done to find different materials to use for the physical breast phantom so that realistic images can be used for the observer study. The investigator found that a 3D computer simulated breast phantom needs to provide a realistic and accurate representation of the breast parenchyma in order to offer a compelling argument for the technique. This can be accomplished through either mathematical methods using geometrical primitives or voxelizations of real patient data. The investigator has decided to use an approach combining empirical breast CT data with subdivision surfaces (SD)and non-uniform rational b-splines (NURBS) in the future for the computer breast simulation.

15. SUBJECT TERMS
Digital Breast Tomosynthesis, Temporal Subtraction, Breast Imaging, Computer Simulation, Phantoms

16. SECURITY CLASSIFICATION OF:			17. LIMITATION OF ABSTRACT	18. NUMBER OF PAGES	19a. NAME OF RESPONSIBLE PERSON
a. REPORT	b. ABSTRACT	c. THIS PAGE			USAMRMC
U	U	U	UU	22	19b. TELEPHONE NUMBER *(include area code)*

Table of Contents

Introduction

This project is to decrease the number of breast cancers that are missed in conventional mammography by combining two methods developed to increase the sensitivity of breast cancer imaging: digital breast tomosynthess (DBT) and temporal subtraction. A major limitation of traditional mammography is the confluence of overlying structures resulting from a two-dimensional (2D) projection of three-dimensional (3D) anatomy. DBT is an exciting new modality for breast imaging which strives to overcome the obstacles presented in conventional 2D mammography by taking multiple projections over a fixed angle and reconstructing volumetric data which serves to isolate overlying anatomy from in-plane structures. Such section images serve to amplify the conspicuity of lesions, particularly in dense breasts. DBT has been shown in several studies to increase the sensitivity of mammography for breast cancer detection. One of the primary methods used by radiologists to detect developing tumors is comparative analysis. This is the process of visually analyzing the temporal change between a current and prior mammogram, utilizing perception to perform the requisite geometric transformation between images. Temporal subtraction is not dissimilar from comparative analysis. It automates the process by using two images taken sequentially and subtracting them in order to find temporal discrepancies. The purpose of this project is to determine the feasibility of using temporal subtraction on DBT phantom images to allow for easier and earlier detection of breast cancer than with either technique alone. A computer simulated phantom will be developed to generate tomosynthesis data sets which can be used for the development and evaluation of an automated registration technique which will then be applied to physical phantom tomosynthesis images in a graphical user interface for the purpose of performing an observer study to asses the developed technique.

Body

Task 1. To generate tomosynthesis datasets of simulated and physical breast phantom, Months 1-12:

1a. Develop a realistic computer simulated breast phantom simulation and generate up to 50 simulated tomosynthesis projection data with the phantom undergoing simulated tissue deformation.

After investigating different types of computer simulated breast phantoms, the investigator believes that a combination of a mathematical and voxelized breast phantom would be the best path to pursue for the computer simulated phantom development. The investigator's colleagues have access to high resolution breast CT datasets that may be used in the phantom development. After seeking the proper institutional approval (e.g. IRB) the investigator plans to segment the breast CT data with an automated segmentation algorithm. The lab of the investigator has a technique which enables the combination of multiple CT datasets into a computer phantom that is flexible in its size and shape called the four dimensional (4D) non-uniform rational b-splines (NURBS) based Cardiac-Torso (NCAT). The segmented data will be utilized to create a detailed 3D computer generated breast phantom based on empirical data using a combination of non-uniform rational b-splines (NURBS) and subdivision surfaces (SD). The phantom will be applicable to many different types of breast imaging research and will be adjustable in size and deformable using finite-element methods. For the purpose of this research project, the 3D computer simulated phantom will provide a realistic and flexible breast phantom for the purpose of registration method development by incorporating simulated compression and the generation of simulated tomosynthesis breast acquisitions.

Issues: The investigator needs to acquire institutional approval to work with human subject data before continuing with this part of the project. After approval, the investigator plans to use some form of adaptive region growing in addition to filtering and thresholding in order to overcome any noise issues and make the algorithm more robust.

1b. Acquire up to 30 tomosynthesis projections of a compressible and deformable physical phantom with physically simulated anatomy and under different simulated temporal discrepancies.

The investigator used a compressible and deformable physical breast phantom shown in Figure 1. Inside of the breast phantom the investigator inserted a number of objects to simulate breast parenchyma: acrylic sponge and yarn (shown in Figure 2) to simulate fibroglandular tissue, differently sized beans and acrylic spheres to simulate nodules (shown in Figure 3), small pieces of egg shell to simulate calcifications, and mineral oil to simulate adipose tissue. The investigator took multiple tomosynthesis exams using 32 kVp, 125 mAs, and with the breast compressed to ~7cm with a slight rotation in-between image acquisitions. There were three scans taken in total: one in the original orientation and original number of simulated lesions; the second with the breast slightly rotated with the original number of simulated lesions; and the third with the breast rotated in a different way and without some of the simulated lesions. Example projections from the compressed phantom are shown in Figure 4.

Figure 1: Compressible and deformable breast phantom

Figure 1: Top – Sponge; Bottom – Acrylic yarn

Issues: The materials used for the physical phantom were not ideal and the tomosynthesis images reconstructed from the acquisition do not look realistic enough to use for the observer study. Further research must be done to match up materials with acquisition parameters to create more realistic images.

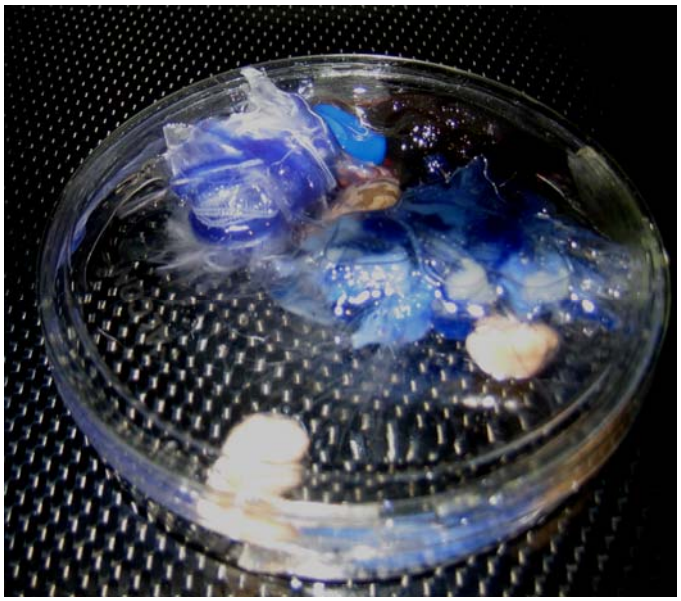

Figure 3: Simulated lesions

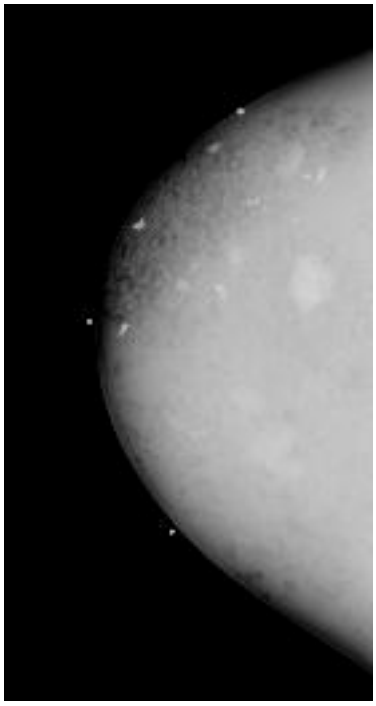

Figure 3: Projection of Physical Phantom

The lab of the investigator has access to a set of DBT human subject images which contain pairs of temporally sequential data. In addition to pursuing the physical phantom pathway, the investigator plans to acquire institutional approval (e.g. IRB) to work with the human subject data. This will give the investigator human data to work with for this project and perhaps lend the technique developed a more compelling clinical and practical implementation.

Issues: IRB approval must be acquired prior to using the temporally sequential human subject DBT images.

The investigator has investigated a simulated dose reduction technique for use on tomosynthesis images using anthropomorphic chest phantom images. This research was performed on chest data in order to continue with prior research and validate the technique on images the investigator had already acquired. We experimentally determined the NPS of the tomosynthesis acquisition system and utilize it to filter an image of random noise. After some further modifications to adjust the noise variance, this resultant noise image is added to the original image and the procedure culminates in an image which simulates an image acquired at a reduced exposure. This technique is easily applicable to the breast tomosynthesis data that the investigator will acquire in the course of this project and can be used to additionally evaluate the dose of breast tomosynthesis images on lesion detectability. Please see Appendix 1 for further details.

Issues: The dose reduction technique that was developed for the chest images must be altered to be used on breast tomosynthesis images.

1c. Utilize up to 3 different tomosynthesis reconstruction algorithms (Filtered Back Projection, Matrix Inversion Tomosynthesis, and Gaussian Frequency Blending) to create tomosynthesis data sets of the simulated and physical phantom.

The DBT images were reconstructed using the Filtered Back Projection algorithm. As mentioned previously the images do not appear to realistically resemble actual breast tomosynthesis images from human subjects. Please see Figure 5 for examples of tomosynthesis slice through the reconstructed volume.

Issues: None.

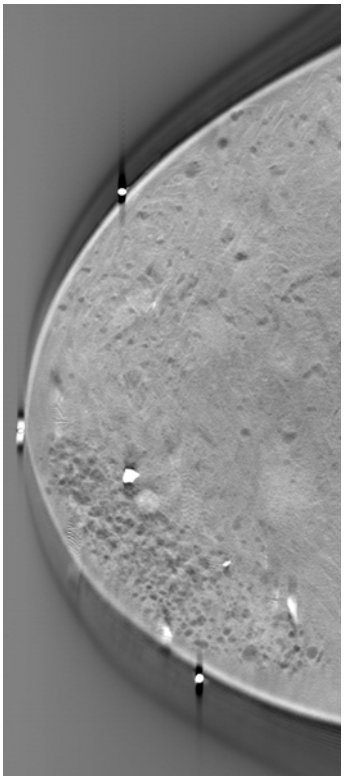

Figure 4: Tomosynthesis slice of physical phantom

Key Research Accomplishments

- Identification of simulation model to use combining real human data and geometric primitives
- Physical breast phantom tomosynthesis images have been acquired and processed
    - New materials must be identified for use in physical breast phantom for more realistic images
- Tomosynthesis simulated dose reduction technique has been developed
    - Needs to be applied to breast images

Reportable Outcomes

1. C. M. Li and J. T. Dobbins, III, "Methodology for Determining Dose Reduction for Chest Tomosynthesis," SPIE Medical Imaging 2007: Physics of Medical Imaging 6510, (2007).

Conclusions

The identification of the proper computer simulation method is an important milestone and will provide a research tool, not only for the scope of this project, but also for use by other institutions who are working on breast imaging. Although further work must be performed towards choosing the correct materials for the physical breast phantom, it was important to show that images could be acquired and they can still be used for the development of the registration algorithm while the computer simulated phantom is being created. DBT has been shown to increase the specificity and sensitivity of lesion detection; however dose reduction is an important addition for clinical implementation of DBT to constrain the radiative dose to the patient during screening. The methodology developed during this project for dose reduction will provide a good simulation technique for evaluating the dose limitations for DBT.

References

[1] S Hofvind, P. Skaane, B. Vitak, H. Wang, S. Thoresen, L. Eriksen, H. Bjorndal, A. Braaten, and N.Bjurstam, "Influence of Review Design on Percentages of Missed Interval Breast Cancers: Retrospective Study of Interval Cancers in a Population-based Screening Program", Radiology **237**, 437 (2005).

[2] Y. Chen, J.Y. Lo, and J. T. Dobbins, III, "Matrix Inversion Tomosynthesis (MITS) of the Breast: Preliminary Results", presented at RSNA, Chicago, IL, 2004.

[3] J. T. Dobbins, III and D. J. Godfrey, "Digital x-ray tomosynthesis: current state of the art and clinical potential", Physics in Medicine and Biology **48** (19), R65 (2003).

[4] L. T. Niklason, B. T. Christian, L. E. Niklason, D. B. Kopans, D. E. Castleberry, B. H. Opsahl-Ong, C.E. Landberg, P. J. Slanetz, A. A. Giardino, R. Moore, D. Albagli, M. C. DeJule, P. F. Fitzgerald, D. F.Fobare, B. W. Giambattista, R. F. Kwasnick, J. Liu, S. J. Lubowski, G. E. Possin, J. F. Richotte, C. Y.Wei, and R. F. Wirth, "Digital tomosynthesis in breast imaging", Radiology **205** (2), 399 (1997).

[5] K. Bliznakova, Z. Bliznakov, V. Bravou, Z. Kolitsi and N. Pallikarakis, "A three-dimensional breast software phantom for mammography simulation," Physics in Medicine and Biology **48**, 3699-3719 (2003).

[6] C. Hoeschen, U. Fill, M. Zankl, et al., "A High-Resolution Voxel Phantom of the Breast for Dose Calculations in Mammography," Radiation Protection Dosimetry **114**, 406-409 (2005).

[7] Y. Chen, J.Y. Lo, and J. T. Dobbins, III, "Impulse response analysis for several digital tomosynthesis mammography reconstruction algorithms", presented at SPIE Medical Imaging: Physics of Medical Imaging, San Diego, 2005.

[8] T. Wu, A. Stewart, M. Stanton, T. McCauley, W. Phillips, D. B. Kopans, R. H. Moore, J. W. Eberhard, B. Opsahl-Ong, L. Niklason, and M. B. Williams, "Tomographic mammography using a limited number of low-dose cone-beam projection images", Medical Physics **30** (3), 365 (2003).

[9] E.A. Sickles, W.N. Weber, H.B. Galvin, S.H. Ominsky, and R.A. Sollitto, "Baseline screening mammography: one vs two views per breast", AJR Am J Roentgenol **147** (6), 1149 (1986).

[10] M.G. Thurfjell, B. Vitak, E. Azavedo, G. Svane, and E. Thurfjell, "Effect on Sensitivity and Specificity of Mammography Screening with or Without Comparison of Old Mammograms", Acta radiologica **41** (1), 52 (2000).

[11] M.P. Callaway, C.R.M. Boggis, S.A. Astley, and I. Hutt, "The influence of previous films on screening mammographic interpretation and detection of breast carcinoma", Clinical Radiology **52** (7), 527 (1997).

[12] E.S. Burnside, E.A. Sickles, R.E. Sohlich, and K.E. Dee, "Differential Value of Comparison with Previous Examinations in Diagnostic Versus Screening Mammography", AJR Am J Roentgenol **179** (5), 1173 (2002).

[13] E.S. Burnside, J.M. Park, J.P. Fine, and G.A. Sisney, "The Use of Batch Reading to Improve the Performance of Screening Mammography", AJR Am J Roentgenol **185** (3), 790 (2005).

[14] T. Ishida, K. Ashizawa, R. Engelmann, S. Katsuragawa, H. MacMahon, and K. Doi, "Application of temporal subtraction for detection of interval changes on chest radiographs: improvement of subtraction images using automated initial image matching", Journal of Digital Imaging **12** (2), 77 (1999).

[15] T. Ishida, S. Katsuragawa, K. Nakamura, H. MacMahon, and K. Doi, "Iterative image warping technique for temporal subtraction of sequential chest radiographs to detect interval change", Med Phys **26** (7), 1320 (1999).

[16] S. Kakeda, K. Nakamura, K. Kamada, H. Watanabe, H. Nakata, S. Katsuragawa, and K. Doi, "Improved detection of lung nodules by using a temporal subtraction technique", Radiology **224** (1), 145 (2002).

[17] A. Kano, K. Doi, H. MacMahon, D. D. Hassell, and M. L. Giger, "Digital image subtraction of temporally sequential chest images for detection of interval change", Med Phys **21** (3), 453 (1994).

[18] C.M. Li and J. T. Dobbins, III, "Preliminary Assessment of the Temporal Subtraction of Tomosynthesis Images for Improved Detection of Pulmonary Nodules", presented at SPIE Medical Imaging 2006: Physics of Medical Imaging, San Diego, CA, 2006.

[19] M. C. Difazio, H. MacMahon, X. W. Xu, P. Tsai, J. Shiraishi, S. G. Armato, 3rd, and K. Doi, "Digital chest radiography: effect of temporal subtraction images on detection accuracy", Radiology **202** (2), 447 (1997).

[20] S. Katsuragawa, H. Tagashira, Q. Li, H. MacMahon, and K. Doi, "Comparison of the quality of temporal subtraction images obtained with manual and automated methods of digital chest radiography", J Digit Imaging **12** (4), 166 (1999).

[21] T. Matsuda, Y. Yasuhara, A. Kano, T. Mochizuki, and J. Ikezoe, "Effect of temporal subtraction technique on the diagnosis of primary lung cancer with chest radiography", Radiat Med **21** (3), 112 (2003).

[22] K. Nakagawa, A. Oosawa, H. Tanaka, and K. Ohtomo, "Clinical Effectiveness of Improved Temporal Subtraction for Digital Chest Radiographs", presented at Medical Imaging 2002: Image Perception, Observer Performance, and Technology Assessment, San Diego, CA, USA, 2002.

[23] L. Hadjiiski, H.P. Chan, B. Sahiner, N. Petrick, and M.A. Helvie, "Automated registration of breast lesions in temporal pairs of mammograms for interval change analysis--local affine transformation for improved localization", Medical Physics **28** (6), 1070 (2001).

[24] L. Hadjiiski, B. Sahiner, H.P. Chan, N. Petrick, M.A. Helvie, and M. Gurcan, "Analysis of temporal changes of mammographic features: Computer-aided classification of malignant and benign breast masses", Medical Physics **28** (11), 2309 (2001).

[25] K. Marias, C. Behrenbruch, S. Parbhoo, A. Seifalian, and M. Brady, "A registration framework for the comparison of mammogram sequences ", IEEE Transactions on Medical Imaging **24** (6), 782 (2005).

[26] S. Van Engeland, P. Snoeren, J. Hendriks, and N. Karssemeijer, "A comparison of methods for mammogram registration", IEEE Transactions on Medical Imaging **22** (11), 1436 (2003).

[27] M.A. Wirth, C. Choi, and A. Jennings, in *IEEE Image Processing and its Applications* (IEEE, Manchester, UK, 1999).

[28] P. Filev, L. Hadjiiski, B. Sahiner, H.P. Chan, and M.A. Helvie, "Comparison of similarity measures for the task of template matching of masses on serial mammograms", Medical Physics **32** (2), 515 (2005).
[29] W. Good, B. Zheng, Y.H. Chang, X. Wang, and G. Maitz, "Generalized procrustean image deformation for subtraction of mammograms", presented at SPIE, San Diego, CA, 1999.
[30] F. Richard, P. Bakic, and A. Maidment, "Mammogram registration: a phantom-based evaluation of compressed breast thickness variation effects", IEEE Transactions on Medical Imaging **25** (2) (2006).
[31] S. Sanjay-Gopal, H. P. Chan, T. Wilson, M. Helvie, N. Petrick, and B. Sahiner, "A regional registration technique for automated interval change analysis of breast lesions on mammograms", Medical Physics **26** (12), 2669 (1999).
[32] S. Timp, S. Van Engeland, and N. Karssemeijer, "A regional registration method to find corresponding mass lesions in temporal mammogram pairs", Medical Physics **32** (8), 2629 (2005).
[33] H P Chan, K Doi, C J Vyborny, R A Schmidt, C E Metz, K L Lam, T Ogura, Y Wu, and H MacMahon, "Improvement in radiologists' detection of clustered microcalcifications on mammograms: The potential of computer-aided diagnosis", Investigative Radiology **25**, 1102 (1990).
[34] H. P. Chan, B. Sahiner, M. A. Helvie, N. Petrick, M. A. Roubidoux, T. E. Wilson, D. D. Adler, C. Paramagul, J. S. Newman, and S. Sanjay-Gopal, "Improvement of radiologists' characterization of mammographic masses by using computer-aided diagnosis: an ROC study", Radiology **212** (3), 817 (1999).
[35] T. Wu, E.A. Rafferty, D.B. Kopans, and R.H. Moore, "Contrast-Enhanced Breast Tomosynthesis-DBT for better breast cancer diagnosis", RT-Image **17** (41) (2004).
[36] A. Carton, S. Chen, M. Albert, E. Conant, M. Schnall, and A. Maidment, "Technical Development of Contrast-enhanced Digital Breast Tomosynthesis", RSNA (2005).
[37] S. Chen, A. Carton, M. Albert, E. Conant, M. Schnall, and A. Maidment, "Initial Experience with Contrast-enhanced Digital Breast Tomosynthesis", RSNA (2005).
[38] J.C. Weinreb and G. Newstead, "MR imaging of the breast", Radiology **196**, 593 (1995). [39] M.D. Schnall, "Breast imaging technology: Application of magnetic resonance imaging to early detection of breast cancer", Breast Cancer Research **3** (1), 17 (2001).
[40] R. Ning, D. Conover, X. Lu, Y. Zhang, Y. Yu, L. Schffhauer, and J. Cullinan, "Evaluation of flat panel detector cone beam CT breast imaging with different sizes of breast phantoms", 2005 Proc. SPIE: Phys. of Med. Imag. **5745** (1), 626 (2005).
[41] J.M Boone, A.L.C. Kwan, T.R. Nelson, N. Shah, G. Burkett, J.A. Seibert, K.K. Lindfors, and G. Ross, "Performance assessment of a pendant-geometry CT scanner for breast cancer detection", 2005 Proc. SPIE: Phys. of Med. Imag. **5745** (1), 319 (2005).
[42] J.M. Boone, T.R. Nelson, K.K. Lindfors, and J.A. Siebert, "Dedicated breast CT: radiation dose and image quality evaluation", Radiology **221** (3), 657 (2001).
[43] R. Ning, Y. Yu, D.L. Conover, X. Lu, H. He, Z. Chen, L. Schiffhauer, and J. Cullinan, "Preliminary system characterization of flat-panel-detector-based cone-beam CT for breast imaging", 2004 Proc. SPIE: Phys. of Med. Imag. **5368** (1), 292 (2004).
[44] A.A. Vedula and S.J. Glick, "Computer simulations of CT mammography using a flat panel imager", 2003 Proc. SPIE: Phys. of Med. Imag. **5030**, 349 (2003).
[45] M.P. Tornai, R.L. McKinley, C.N. Brzymialkiewicz, P. Madhav, S.J. Cutler, D.J. Crotty, J.E. Bowsher, E. Samei, and C.E. Floyd, "Design and development of a fully-3D dedicated x-ray computed mammotomography system", 2005 Proc. SPIE: Phys. of Med. Imag. **5745** (1), 189 (2005).
[46] R.L. McKinley, M.P. Tornai, C.N. Brzymialkiewicz, E. Samei, and J.E. Bowsher, "Analysis of a novel offset cone-beam computed mammotomography imaging system for attenuation correction of SPECT in a proposed dual modality dedicated breast mammotomography system", presented at *2004 Workshop on the Nuclear Radiology of the Breast*, Rome, Italy, 2004.
[47] B. Chen and R. Ning, "Cone-beam volume CT mammographic imaging: feasibility study", Med. Phys. **29** (5), 755 (2002).
[48] L. Chen, C.C. Shaw, S. Tu, M.C. Altunbas, T. Wang, C. Lai, X. Liu, and S.C. Kappadath, "Cone-beam CT breast imaging with a flat panel detector: a simulation study", 2005 Proc. SPIE: Phys. of Med. Imag. **5745** (1), 943 (2005).
[49] B. Fischer and J. Modersitzki, "Combination of automatic non-rigid and landmark based registration: the best of both worlds", presented at Medical Imaging 2003: Image Processing, 2003.
[50] J.B.A. Maintz and M.A. Viergever, "A survey of medical image registration", Medical Image Analysis **2** (1), 1 (1998).
[51] C.R. Meyer, J.L. Boes, B. Kim, H.P. Bland, K.R. Zasadny, P.V. Kison, K. Koral, K. Frey, and R.L. Wahl, "Demonstration of accuracy and clinical versatility of mutual information for automatic multimodality image fusion using affine and thin-plate spline warped geometric deformations", Medical Image Analysis **1** (3), 195 (1997).
[52] T. Rohlfing, C.R. Maurer, Jr., D.A. Bluemke, and M.A. Jacobs, "Volume-preserving nonrigid registration of MR breast images using free-form deformation with an incompressibility constraint", IEEE Transactions on Medical Imaging **22** (6), 730 (2003).
[53] K. Rohr, H.S. Stiehl, R. Springel, T.M. Buzug, J. Weese, and M.H. Kuhn, "Landmark-based elastic registration using approximating thin-plate splines", IEEE Transactions on Medical Imaging **20** (6), 526 (2001).
[54] D. Rueckert, C. Hayes, C. Studholme, P. Summers, M.O. Leach, and D.J. Hawkes, "Non-rigid Registration of Breast MR Images Using Mutual Information", presented at First International Conference on Medical Image Computing and Computer-Assisted Intervention, 1998.
[55] D. Rueckert, L.I. Sonoda, C. Hayes, D.L.G. Hill, M.O. Leach, and D.J. Hawkes, "Nonrigid registration using free-form deformations: Applications to breast MR images", IEEE Transactions on Medical Imaging **18** (8), 712 (1999).
[56] R. Sivaramakrishna, "3D breast image registration - a review", Technology in Cancer REsearch & Treatment **4** (1), 39 (2005).
[57] F. Maes, A. Collignon, D. Vandermeulen, G. Marchal, and P Suetens, "Multimodality image registration by maximization of mutual information", IEEE Transactions on Medical Imaging **16** (2), 187 (1997).
[58] M.H. Davis, A. Khotanzad, D.P. Flamig, and S.E. Harms, "A physics-based coordinate transformation for 3-D image matching", IEEE Transactions on Medical Imaging **16** (3), 317 (1997).

[59] Y. Chen, J.Y. Lo, J.A. Baker, and J. T. Dobbins, III, "Gaussian frequency blending algorithm with Matrix Inversion Tomosynthesis (MITS) and Filtered Back Projection (FBP) for better digital breast tomosynthesis reconstruction", presented at SPIE Medical Imagng: Physics of Medical Imaging, San Diego, CA, 2006.
[60] Y. Chen, J.Y. Lo, J.A. Baker, and J. T. Dobbins, III, "Noise power spectrum analysis for several digital breast tomosynthesis reconstruction algorithms", presented at SPIE Medical Imaging: Physics of Medical Imaging, San Diego, CA, 2006.
[61] L A Feldkamp, L C Davis, and J W Kress, "Practical cone-beam algorithm", Journal of the Optical Society of America **1**, 612 (1984).
[62] J. T. Dobbins, III, D. J. Godfrey, and H. P. McAdams, *Chest tomosynthesis. In Advances in Digital Radiography: RSNA Categorical course in Digital Radiography*. (Radiological Society of North America, Oak Brook, Illinois, 2003).
[63] J. T. Dobbins, III, A. O. Powell, and Y. K. Weaver, "Matrix Inversion Tomosynthesis: initial image reconstruction", presented at RSNA 73rd Scientific Assembly, Chicago, Illinois, 1987.
[64] J. T. Dobbins, III, R. L. Webber, and S. M. Hames, "Tomosynthesis for improved pulmonary nodule detection", presented at RSNA 84th Scientific Assembly, Chicago, Illinois, 1998.
[65] D. J. Godfrey and J. T. Dobbins, III, "Optimization of Matrix Inversion Tomosynthesis via impulse response simulations", presented at RSNA 88th Scientific Assembly, Chicago, IL, 2002.
[66] D. J. Godfrey, A. Rader, and J. T. Dobbins, III, "Practical strategies for the clinical implementation of matrix inversion tomosynthesis (MITS)", presented at Medical Imaging 2003: Physics of Medical Imaging Conference, 2003.
[67] D. J. Godfrey, R. J. Warp, and J. T. Dobbins, III, "Optimization of Matrix Inverse Tomosynthesis", presented at Proceedings of SPIE, 2001.
[68] D. J. Godfrey, R. J. Warp, and J. T. Dobbins, III, "Optimization of noise attributes in matrix inversion tomosynthesis", presented at RSNA 87th Scientific Program, Chicago, IL, 2001.
[69] R. J. Warp, D. J. Godfrey, and J. T. Dobbins, III, "Applications of Matrix Inverse Tomosynthesis", presented at Proceedings of SPIE, 2000.
[70] P. Bakic, M. Albert, D. Brzakovic, and A. Maidment, "Mammogram synthesis using a 3D simulation. I. Breast tissue model and image acquisition simulation", Medical Physics **29** (9), 2131 (2002).
[71] P. Bakic, M. Albert, D. Brzakovic, and A. Maidment, "Mammogram synthesis using a 3D simulation. II. Evaluation of synthetic mammogram texture", Medical Physics **29** (9), 2140 (2002).
[72] F O Bochud, C K Abbey, and M P Eckstein, "Statistical texture synthesis of mamographic images with clustered lumpy backgrounds", Optics Express **4** (1), 33 (1999).
[73] X. Gong, S.J. Glick, B. Liu, A.A. Vedula, and S. Thacker, "A computer simulation study comparing lesion detection accuracy with digital mammography, breast tomosynthesis, and cone-beam CT breast imaging", Medical Physics **33** (4), 1041 (2006).
[74] R.A. Hunt, D.R. Dance, P.R. Bakic, A. Maidment, M. Sandborg, G. Ullman, and G. Alm Carlsson, "Calculation of the properties of digital mammograms using a computer simulation", Radiation Protection Dosimetry **114**, 395 (2005).
[75] P. Bakic, M. Albert, D. Brzakovic, and A. Maidment, "Mammogram synthesis using a threedimensional simulation. III. Modeling and evaluation of the breast ductal network", Med Phys **30** (7), 1914 (2003).
[76] T. Wu, R. H. Moore, E. A. Rafferty, and D. B. Kopans, "A comparison of reconstruction algorithms for breast tomosynthesis", Medical Physics **31** (9), 2636 (2004).
[77] C. Studholme, D.L.G. Hill, and D.J. Hawkes, "An overlap invariant entropy measure of 3D medical image alignment", Pattern Recognition **32** (1), 71 (1999).
[78] V. Pekar, E. Gladilin, and K. Rohr, "An adaptive irregular grid approach for 3D deformable image registration", Physics in Medicin and Biology **51**, 361 (2006).
[79] F.L. Bookstein, "Principal warps: thin-plate splines and the decomposition of deformations", Ieee Transactions on Pattern Analysis and Machine Intelligence **11** (6), 567 (1989).
[80] G.E. Christensen, R.D. Rabbitt, and M.I. Miller, "3D brain mapping using a deformable neuroanatomy", Physics in Medicine and Biology **39**, 609 (1994).
[81] M.I. Miller, G.E. Christensen, Y. Amit, and U. Grenander, "Mathematical textbook of deformable neuroanatomies", Proceedings of the National Academy of Sciences **90**, 11944 (1993).
[82] J.D. Foley and A. Van Dam, *Fundamentals of interactive computer graphics*. (Addison-Wesley Longman Publishing Co., Inc., Boston, MA, 1982).
[83] C.E. Metz, B.A. Herman, and C.A. Roe, "Statistical comparison of two ROC-curve estimates obtained from partially-paired datasets", Med Decis Making **18** (1), 110 (1998).
[84] I. Reiser, R.M. Nishikawa, M. L. Giger, T. Wu, E. Rafferty, R.H. Moore, and D. Kopans, "Computerized mass detection for digital breast tomosynthesis directly from the projection images", Med Phys **33** (2), 482 (2006).
[85] I. Reiser, R. M. Nishikawa, M. L. Giger, T. Wu, E. Rafferty, R. H. Moore, and D. B. Kopans, "Computerized detection of mass lesions in digital breast tomosynthesis images using two- and three dimensional radial gradient index segmentation", Technology in Cancer Research & Treatment **3** (5), 437 (2004).
[86] L. Li, Y. Chu, X. Hu, M. Kallergi, J.A. Thomas, R.A. Clark, J.W. Eberhard, and B.E.H. Claus, "3D object localization and visualization in breast tomosynthesis", Digital Mammography, 202 (2002).
[87] H.P. Chan, J. Wei, B. Sahiner, E. Rafferty, T. Wu, M.A. Roubidoux, R.H. Moore, D. Kopans, L. Hadjiiski, and M.A. Helvie, "Computerized detection of masses on digital tomosynthesis mammograms", Digital Mammography (2004).
[88] H.P. Chan, J. Wei, B. Sahiner, E. Rafferty, T. Wu, M.A. Roubidoux, R.H. Moore, D. Kopans, M. Lubomir, L. Hadjiiski, and M.A. Helvie, "Computer-aided Detection System for Breast Masses on Digital Tomosynthesis Mammograms: Preliminary Experience", Radiology **237**, 1075 (2005).

[89] M. Kallergi, W. Qian, J.A. Thomas, J.W. Eberhard, B.E.H. Claus, and R.A. Clark, "CAD methodology transfer from 2D to 3D digital mammography for calcification enhancement and segmentation: A feasibility study", Digital Mammography (2002).
[90] W. P. Segars, "Development and application of the new dynamic NURBS-based cardiac-torso (NCAT) phantom," Dissertation, University of North Carolina, 2001
[91] W. P. Segars, D. S. Lalush and B. M. W. Tsui, "Modeling respiratory mechanics in the MCAT and spline-based MCAT phantoms," Ieee Transactions on Nuclear Science **48**, 89-97 (2001).
[92] W. P. Segars, D. S. Lalush and B. M. W. Tsui, "A realistic spline-based dynamic heart phantom," Ieee Transactions on Nuclear Science **46**, 503-506 (1999).
[93] W. P. Segars, M. Mahesh, T. Beck, E. C. Frey and B. M. W. Tsui, "Validation of the 4D NCAT simulation tools for use in high-resolution x-ray CT research," SPIE Medical Imaging Conference (2005).
[94] W. P. Segars and B. M. W. Tsui, "Study of the efficacy of respiratory gating in myocardial SPECT using the new 4-D NCAT phantom," Ieee Transactions on Nuclear Science **49**, 675-679 (2002).
[95] F. Richard, P. Bakic and A. Maidment, "Mammogram registration: a phantom-based evaluation of compressed breast thickness variation effects.," IEEE Trans Med Imag **25**, 188-197 (2006).
[96] O. Tischenko, C. Hoeschen, D. Dance, et al., "Evaluation of a novel method of noise reduction using computer-simulated mammograms," Radiation Protection Dosimetry **114**, 81-84 (2005).
[97] R. A. Hunt, D. R. Dance, P. R. Bakic, et al., "Calculation of the properties of digital mammograms using a computer simulation," Radiation Protection Dosimetry **114**, 395-398 (2005).
[98] E. Samei, M. J. Flynn and W. R. Eyler, "Detection of Subtle Lung Nodules: Relative Influence of Quantum and Anatomical Noise on Chest Radiographs," Radiology **213**, 727-734 (1999).
[99] R. S. Saunders, E. Samei and C. Hoeschen, "Impact of Resolution and Noise Characteristics of Digital Radiographic Systems on the Detectability of Lung Nodules," SPIE Medical Imaging 2003: Image Processing **Proc. SPIE (in press)**, (2003).
[100] L. Zhou, J. Oldan, P. Fisher and G. Gindi, "Low-Contrast Lesion Detection in Tomosynthetic Breast Imaging Using a Realistic Breast Phantom," SPIE Medical Imaging: Physics of Medical Imaging **6142**, (2006).
[101] J. Zhou, B. Zhao and W. Zhao, "A Computer simulation platform for the optimization of a breast tomosynthesis system," Medical Physics **34**, 1098-1109 (2007).
[102] J. Shorey, "Stochastic Simulations for the Detection of Objects in Three Dimensional Volumes: Applications in Medical Imaging and Ocean Acoustics," PhD Dissertation, Duke University, 2007
[103] F. S. Azar, D. N. Metaxas and M. D. Schnall, "A Deformable Finite Element Model of the Breast for Predicting Mechanical Deformations under External Perturbations," Acadamic Radiology **8**, 965-975 (2001).
[104] J. M. Boone, A. L. Kwan, K. Yang, et al., "Computed tomography for imaging the breast," Journal of Mammary Gland Biology and Neoplasia **11**, 103-111 (2006).
[105] K. Yang, A. L. Kwan and J. M. Boone, "Computer modeling of the spatial resolution properties of a dedicated breast CT system," Medical Physics **34**, 2059-2069 (2007).
[106] L. Piegl, "On NURBS: a survey," IEEE Computer Graphics and Applications **11**, 55-71 (1991).
[107] L. Piegl and W. Tiller, *The Nurbs Book*, (Springer-Verlag, New York, 1997).
[108] H. Hoppe, T. DeRose, T. Duchamp, et al., "Piecewise smooth surface reconstruction," Computer Graphics **28**, 295-302 (1994).
[109] C. Tanner, J. A. Schnabel, D. L. Hill, et al., "Factors influencing the accuracy of biomechanical breast models," Medical Physics **33**, 1758-1769 (2006).
[110] A. Samani, J. Bishop, M. J. Yaffe and D. B. Plewes, "Biomechanical 3-D finite element modeling of the human breast using MRI data," IEEE Transactions on Medical Imaging **20**, 271-279 (2001).
[111] D. N. Ghista, A. S. Kobayashi, N. Davis and G. Ray, "Finite element analysis in biomechanics," International Conference on Variational Methods in Engineering **5**, 50-81 (1973).
[112] D. P. Frush, C. C. Slack, C. L. Hollingsworth, et al., "Computer-Simulated Radiation Dose Reduction for Abdominal Multidetector CT of Pediatric Patients," American Journal of Roentgenology **179**, 1107-1113 (2002).
[113] M. Volk, O. W. Hamer, S. Feuerbach and M. Strotzer, "Dose reduction in skeletal and chest radiography using a large-area flat-panel detector based on amorphous silicon and thallium-doped cesium iodide: technical background, basic image quality parameters, and review of the literature," European Radiology **14**, 827-834 (2004).
[114] A. J. Britten, M. Crotty, H. Kiremidjian, A. Grundy and E. J. Adam, "The addition of computer simulated noise to investigate radiation dose and image quality in images with spatial correlation of statistical noise: an example application to X-ray CT of the brain," The British Journal of Radiology **77**, 323-328 (2004).
[115] J. R. Mayo, K. P. Whittall, A. N. Leung, et al., "Simulated Dose Reduction in Conventional Chest CT: Validation Study," Radiology **202**, 453-457 (1997).
[116] M. Bath, M. Hakansson, A. Tingberg and L. G. Mansson, "Method of Simulating Dose Reduction for Digital Radiographic Systems," Radiation Protection Dosimetry **114**, 253-259 (2005).
[117] R. S. Saunders and E. Samei, "A method for modifying the image quality parameters of digital radiographic images," Medical Physics **30**, 3006-3017 (2003).
[118] International Electrotechnical Commission, *Medical diagnostic X-ray equipment - Radiation conditions for use in the determination of characteristics*, (Geneva, Switzerland, 2005).
[119] R. S. Saunders, E. Samei, J. L. Jesneck and J. Y. Lo, "Physical characterization of a prototype selenium-based full-field digital mammography detector," Medical Physics **32**, 588-599 (2005).
[120] J. T. Dobbins, III, E. Samei, N. T. Ranger and Y. Chen, "Intercomparison of methods for image quality characterization. II. Noise power spectrum," Medical Physics **33**, 1466-1475 (2006).

Appendix 1

1. C. M. Li and J. T. Dobbins, III, “Methodology for Determining Dose Reduction for Chest Tomosynthesis,” SPIE Medical Imaging 2007: Physics of Medical Imaging 6510, (2007).

Methodology for Determining Dose Reduction for Chest Tomosynthesis

Christina M. Li [1,2], James T. Dobbins III [1,2,3,4]

[1]Department of Biomedical Engineering, Duke University, Durham, NC 27710
[2]Duke Advanced Imaging Laboratories, Duke University Medical Center, Durham, NC 27710
[3]Department of Radiology, Duke University Medical Center, Durham, NC 27710
[4]Medical Physics Graduate Program, Duke University, Durham, NC 27710

Digital tomosynthesis is an imaging technique that reconstructs tomographic planes in an object from a set of projection images taken over a fixed angle[1]. Preliminary results show that this technique increases the detectability of lung nodules[2]. Current settings acquire images with approximately the same exposure as a screen-film lateral. However, due to the increased detectability of lung nodules from the removal of overlying structures, patient dose may be reduced while still maintaining increased sensitivity and specificity over conventional chest radiographs. This study describes a simulation method that provides realistic reduced dose images by adding noise to digital chest tomosynthesis images in order to simulate lower exposure settings for the purpose of dose optimization. Tomosynthesis projections of human subjects were taken at dose levels which were specified based on either patient thickness or a photo-timed digital chest radiograph acquired prior to tomosynthesis acquisition. For the purposes of this study, subtle nodules of varying size were simulated in the image for demonstration purposes before the noise simulation in order to have a known truth for nodule location and to evaluate the effect of additive noise on tumor detection. Noise was subsequently added in order to simulate ¾, ½, and ¼ of the original exposure in each projection. The projections were then processesed with the MITS algorithm to produce slice images. The subjective assessment of the resulting tomosynthesis slice images show a potential decrease in dose level by 25-50%. This method will be applied to a study of dose reduction in the future using human subject cases.

Keywords: digital x-ray imaging (DX), tomsynthesis (RECON), x-ray tomosynthesis (TSYN), simulation (SIM)
Preferred Presentation Type: Oral Presentation
Conference Code: MI03 - Physics of Medical Imaging.

Introduction

There has been much interest in dose optimization for radiography in order to reduce patient exposure while maintaining adequate image quality for diagnosis. However, to our knowledge, this subject has not yet been addressed for digital chest tomosynthesis imaging. Much of the misdiagnosis in projection radiography is due to anatomic noise from overlying structures. Digital tomosynthesis is a method which reconstructs longitudinal planes within a patient from a set of digital projection images taken over a limited angle. Tomosynthesis increases detectability of abnormalities by removing the overlying anatomy and improving the conspicuity of in-plane structures. Although tomosynthesis has been around for many decades, it has only recently become clinically practical with the advent of flat-panel detector technology. In a pilot study performed in our lab, 50% of CT confirmed nodules were found in the PA chest radiograph versus 81% in a tomosynthesis image set[2]. The current default dose setting for our tomosynthesis imaging system is roughly equivalent to a screen-film lateral. This was chosen because of the similarity in image quality of tomosynthesis images taken at this exposure to conventional chest radiographs. There is potential to lower tomosynthesis exposures because the conspicuity of nodular opacities in the tomosynthesis images at the current default dose setting is not likely limited by x-ray quantum noise. Thus, the increased detectability of abnormalities provided by tomosynthesis may decrease the need for the default dose setting which gives the appearance of a traditional exposure. In previous studies, the addition of computer simulated noise to real human data has been implemented as a way to investigate the diagnostic accuracy as a function of dose reduction[3-8]. The methodology discussed in this work provides a realistic simulation of lower exposure by adding stochastic noise that has been filtered by the characteristic noise power spectrum (NPS) of the system to the projection images prior to tomosynthesis reconstruction. For the purpose of this study, the use of additional simulated lung nodules serves to provide a larger sample size than available with CT confirmed nodules as well as the ability to place them in obscured and un-obscured regions to in order to evaluate the effect of exposure on nodule detection.

Methods

The ultimate purpose of this methodology is to simulate an image acquired at a reduced dose with our imaging system. In order to simulate noise on previous acquired data, which realistically emulates the actual noise of the system, many steps had to be taken. The noise power spectrum (NPS) is one of the most common metrics which describe the noise properties of imaging system. We experimentally determined the NPS of the tomosynthesis acquisition system and utilize it to filter an image of random noise. This noise is added, after some further modifications, to the original image and the procedure results in an image which simulates an image acquired at a reduced exposure.

NPS measurement:

In order to characterize the noise properties of the tomosynthesis system, the noise power spectrum (NPS) was determined experimentally. In the spatial frequency domain, the NPS is the variance per frequency bin of a stochastic signal. In order to correct for the gain of the system, the NPS is divided by the square of the mean pixel value of the area under analysis. This is commonly called the normalized noise power spectrum (NNPS))[10, 11].

$$NNPS(u,v) = NPS(u,v) / (large\ area\ signal)^2 \qquad (1)$$

A previously published method was utilized to calculate and determine the NNPS[10, 11].

At each dose specified, we acquired ten tomosynthesis image sets which gave us 10 flat field image projections for each angle. At each angle, the ten flat field images were averaged together in order to create an image which contained the structural noise inherent in the imaging system. This averaged image set was subtracted from one of the ten original image sets in order to remove any artifactual background shading which would influence the NPS measurement. This background subtracted image set was utilized for all NPS measurement. In order to account for the alteration in variance due to the image subtraction, the resultant NNPS from this methodology was multiplied by *N/N-1*.

A 640×640 pixel area in the center of each background subtracted image, segmented into 128×128 overlapping regions of interest (ROI) was used for analysis. In order to account for small variations in regional exposure over the flat field image, each ROI was scaled by a ratio of its mean pixel value and the mean value of a designated ROI.

According to Saunders *et al*.[10] the NNPS is defined according to the following relation:

$$NNPS = \frac{dA}{M \cdot N^2} \sum_{i=1}^{M} \left\{ \frac{\langle ROI_i \rangle}{\langle ROI_I \rangle} \left| FFT\left[\frac{1}{\langle ROI_i \rangle} \left(ROI_i - \langle ROI_i \rangle \right) \right] \right|^2 \right\} \qquad (2a)$$

Where dA is the pixel area, M is the number of regions used for analysis, N is the number of pixels along one edge of an ROI, ROI_i is a region of interest in the area under analysis, ROI_1 is the ROI in the top left corner of the area under analysis, and $<ROI_i>$ was the mean of ROI_i.

Since we found experimentally that the NNPS did not vary greatly between the different projections, we averaged all of the projections in order to give the final NNPS measurement for the dose under analysis. For the tomosynthesis NNPS measurement, the NNPS was calculated as above for each projection image and the average NNPS was used for the rest of our routine.

$$NNPS_T = \frac{1}{K} \sum_{j=1}^{K} NNPS_j \qquad (2b)$$

$NNPS_j$ is the NNPS from a single projection image, and K is the number of projections.

Noise simulation

In order to create additive noise which has the same noise properties as the true projection images, the texture of the noise must be adjusted according to the experimentally determined $NNPS_T$. The $NNPS_T$, from only one dose was used to filter the noise for all dose levels because the shape of the $NNPS_T$ was found to be relatively consistent at the range of exposures measured. A polynomial curve fit was applied to the $NNPS_T$ and this was utilized to create a radially symmetric estimated $NNPS_T$ ($<NNPS_T>$). The square root of this two dimensional $<NNPS_T>$ is multiplied by the two-dimensional FFT of an uncorrelated Gaussian noise array with zero mean and unit variance. The noise image is then converted back into the spatial domain by taking the inverse FFT. The resulting filtered noise now has frequency content consistent with the tomosynthesis imaging system. Before adding the filtered noise image to the original image ($I_{original}$), the variance of the noise has to be adjusted so that the resultant image ($I_{simulated}$) has a signal to noise ratio (SNR) consistent with a reduced dose image.

As radiation dose decreases, the SNR of the image also decreases. However, since we are utilizing previously acquired clinical data, there is no way to decrease the dose experimentally in order to find the SNR of a reduced dose image. Therefore, we added an image containing filtered noise (I_{noise}) to the original projection image ($I_{original}$) that decreased the SNR appropriately to achieve the target reduced SNR ($SNR_{reduced}$). The result is an image which simulates a reduced exposure ($I_{simulated}$).

$$I_{simulated} = I_{original} + I_{noise} \tag{3}$$

The target SNR cannot be achieved without considering the noise already present in the original image ($I_{original}$). Therefore, because variances add for sums of uncorrelated random variables, the required variance to simulate a lower exposure can be calculated.

$$\sigma^2_{simulated} = \sigma^2_{original} + \sigma^2_{noise} \tag{4}$$

The relationship between variance in the image (σ^2) and the mean pixel intensity ($< I >$) was experimentally determined in order to account for the spatial variation in photon flux. From this relationship, we derived that SNR varies as a function of exposure ($snr(E)$). This was done assuming that the expected pixel value of the image ($< I >$) is proportional to exposure in a linear, quantum-limited detector.

$$SNR_{original} = \frac{< I_{orig} >}{\sigma_{orig}} = snr(E_{original}) \tag{5a}$$

$$SNR_{reduced} = snr(E_{reduced}) \tag{5b}$$

Because we are adding noise to the original image in order to attain a reduced SNR, we can solve for the additive noise variance.

$$\frac{< I_{orig} >}{\sigma_{simulated}} = SNR_{reduced} \tag{6}$$

$$\left(\frac{< I_{orig} >}{SNR_{reduced}} \right)^2 = \sigma^2_{original} + \sigma^2_{noise} \tag{7}$$

$$\sqrt{\left(\frac{< I_{orig} >}{SNR_{reduced}}\right)^2 - \sigma^2_{original}} = \sigma_{noise} \qquad (8)$$

The filtered noise is multiplied by the variance determined from Equation 8. This process adjusts I_{noise} for a spatial variance consistent with the local pixel intensity in the original image in order to account for varying attenuation from different anatomical structures. This process results in a final noise image I_{noise} which contains the same frequency content as the inherent system noise and is also adjusted for the local spatial variations in exposure. This final I_{noise} is added to $I_{original}$ to create the reduced exposure projection image $I_{simulated}$ which has and SNR equal to $SNR_{reduced}$.

Nodule Simulation:

In each set of projections, five subtle lung nodules ranging from 4 to 8 mm in diameter were simulated at different locations in the left lung on the original projection images[12, 13]. The locations of the nodules were chosen carefully to evaluate the effect of exposure level on the detectability of nodules under various anatomical conditions: mediastinum, vessel crossings, and behind ribs. The location of each simulated nodule on each projection imagewas calculated using the fractional angular displacement from horizontal (0° is located at projection 36). The resulting projections with five simulated nodules were then passed into the aforementioned noise simulation routine. Nodule simulation is for demonstration purposes only. It is utilized to have a known truth of tumor location and to evaluate the effect of dose reduction on nodule detection; but is not necessary for the typical application of this methodology to assess the clinical detection performance of reduced dose tomosynthesis images.

Acquisition method

A prototype system constructed in our laboratory with a commercial-grade 41×41 cm a:Si/CsI flat-panel radiographic detector(GE Healthcare, Milwaukee, WI) and rapid acquisition hardware was utilized for all measurements and image acquisition. NPS measurement was done in accordance with the International Electrotechnical Commission (IEC) standard of measurement (IEC 61267 Ed. 2.0 b:2005; RQA9 technique)[9] slightly adjusted for tomosynthesis image acquisition. The antiscatter grid, system faceplate, and 0.2 mm of Cu filtration were kept in place for system calibration and NPS measurement. Beam quality was achieved with 120 kV and 39.9 mm Al filtration (half-value layer of 11.5 mm). All flat field image sets and exposure measurements were made with the standard tomosynthesis acquisition procedure which utilizes 71 projection images over 20 degrees and acquired at 6.4 frames per second with the manufacturer supplied gain and offset corrections applied. All images were acquired with 39.9 mm of Al and 0.2mm of Cu filtration in place. Measurements were made at four exposure levels using: 0.32, 0.4, 0.64, and 1.25 mAs/projection.

Due to the geometry of the system, it was not possible to place the ionization chamber (MDH Model 1015, 10X5-6 ionization chamber, Radcal, Monrovia, CA) in the beam during acquisition of the NPS images. Therefore, the cumulative exposure at each dose level for all 71 projections was measured at the plane of the detector utilizing a small field of view, after the NPS image acquisitions for each dose were completed.

In order to give examples of how this dose reduction simulation method performs, tomosynthesis datasets were acquired of real human subjects at 120 kVp and an mAs setting which was determined based upon either subject thickness or a photo-timed value using the Automatic-Exposure Control (AEC) from a clinical digital chest radiograph unit (GE Healthcare, Milwaukee WI). The range of mAs values was 0.32 to 1 mAs per projection.

After nodule and noise simulation, 69 planes were reconstructed from each set of the projections with simulated noise and nodules using the MITS (Matrix Inversion Tomosynthesis) algorithm [14, 16] developed in our lab, with 5 mm plane spacing. A sliding average of 7 adjacent planes was used to improve image noise and resulted in the final image set which was utilized for the analysis of the simulated dose reduction method.

Results

The normalized NPS (NNPS) from four different dose levels, which are representative of what are used during clinical acquisition, were analyzed: 0.32, 0.4, 0.64, and 1.25 mAs per projection, with the cumulative exposure from a full tomosynthesis acquisition of: 1.83, 2.35, 3.85, and 7.8 mR respectively. Figure 1a. shows that the shape NNPS did not vary greatly at different projections and therefore we averaged them to form the composite NNPS ($NNPS_T$,) for each dose. A fifth order polynomial curve fit was utilized to estimate an equation for the $NNPS_T$. The resultant fit is shown in Figure 1b. along with the $NNPS_T$. Figure 1c shows the NNPS from one projection angle (0º) for each of the dose levels. Figure 1d demonstrates that the system has a very low level of electronic noise because the product of NNPS and exposure does not vary greatly over the range of exposures evaluated.

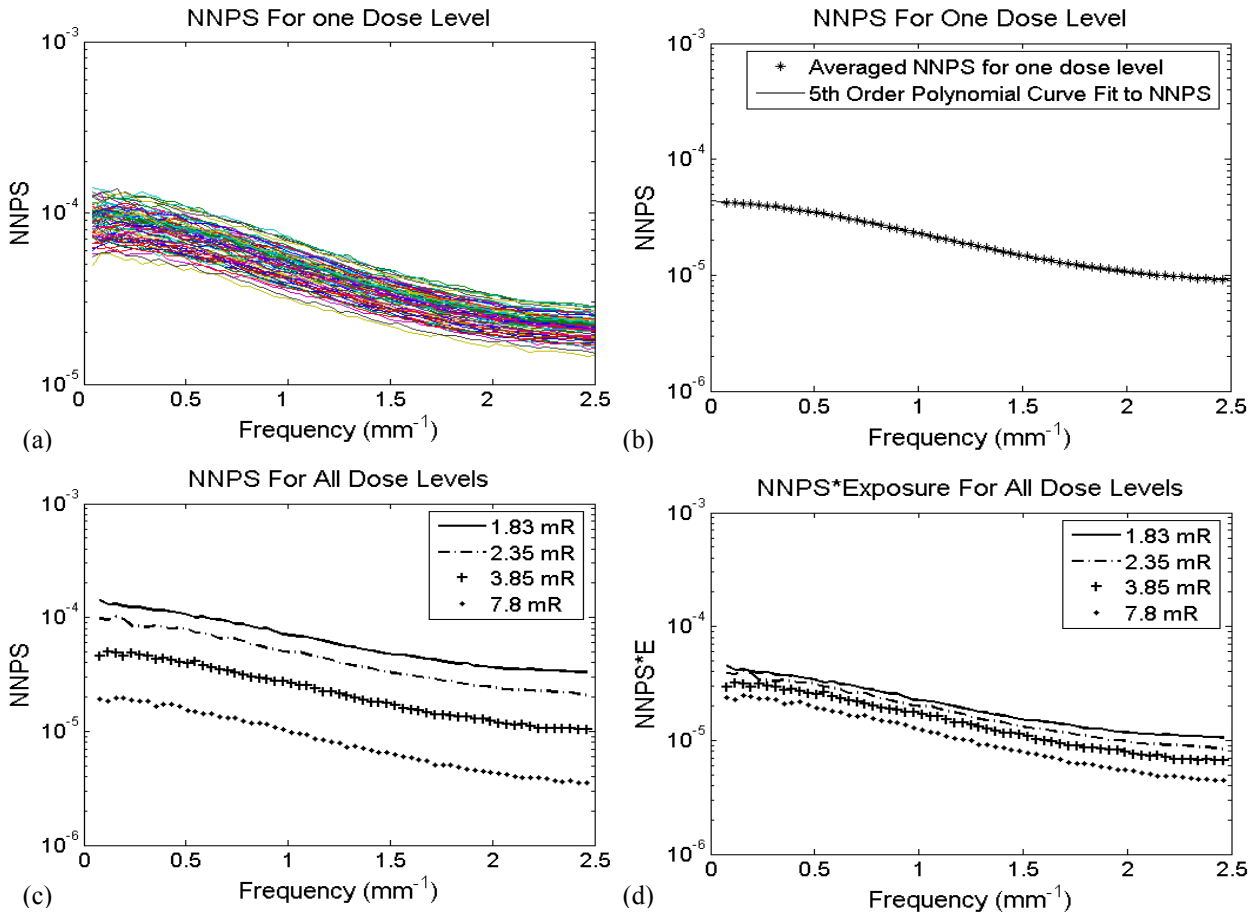

Figure 1: (a) Ensemble of normalized NPS (NNPS) curves from one dose acquisition of all 71 projection images. (b) The averaged NNPS curve from one dose acquisition with the associated curve fit. (c) Example NNPS of all four exposures. (d) The NNPS multiplied by the exposure level (curves would all be the same if the detector was quantum-limited).

The linearity of the detector was found by computing the spatial mean and variance of the flat field projections utilizing the central 80% of the image for each exposure level. (Note: Variance was determined from flat field projections with the background subtracted and corrected with N/N-1). Using this relationship, the amount of noise in the reduced dose image is computed for each pixel. In our methodology, we utilize the characteristic response curves of the system shown in Figure 2a in order to estimate the relative exposure level in each pixel of the clinical image set. From this relationship, we utilize the relationship between the SNR and exposure level and can determine the SNR at the target dose level. Figure 2 (a,c,e) demonstrate these empirically derived relationships. From Figure 2 (b,d) it can be seen that these relationships are not highly dependent on projection angle. We averaged the mean and variance over all projection angles in order to derive the relationships for the system performance due to exposure.

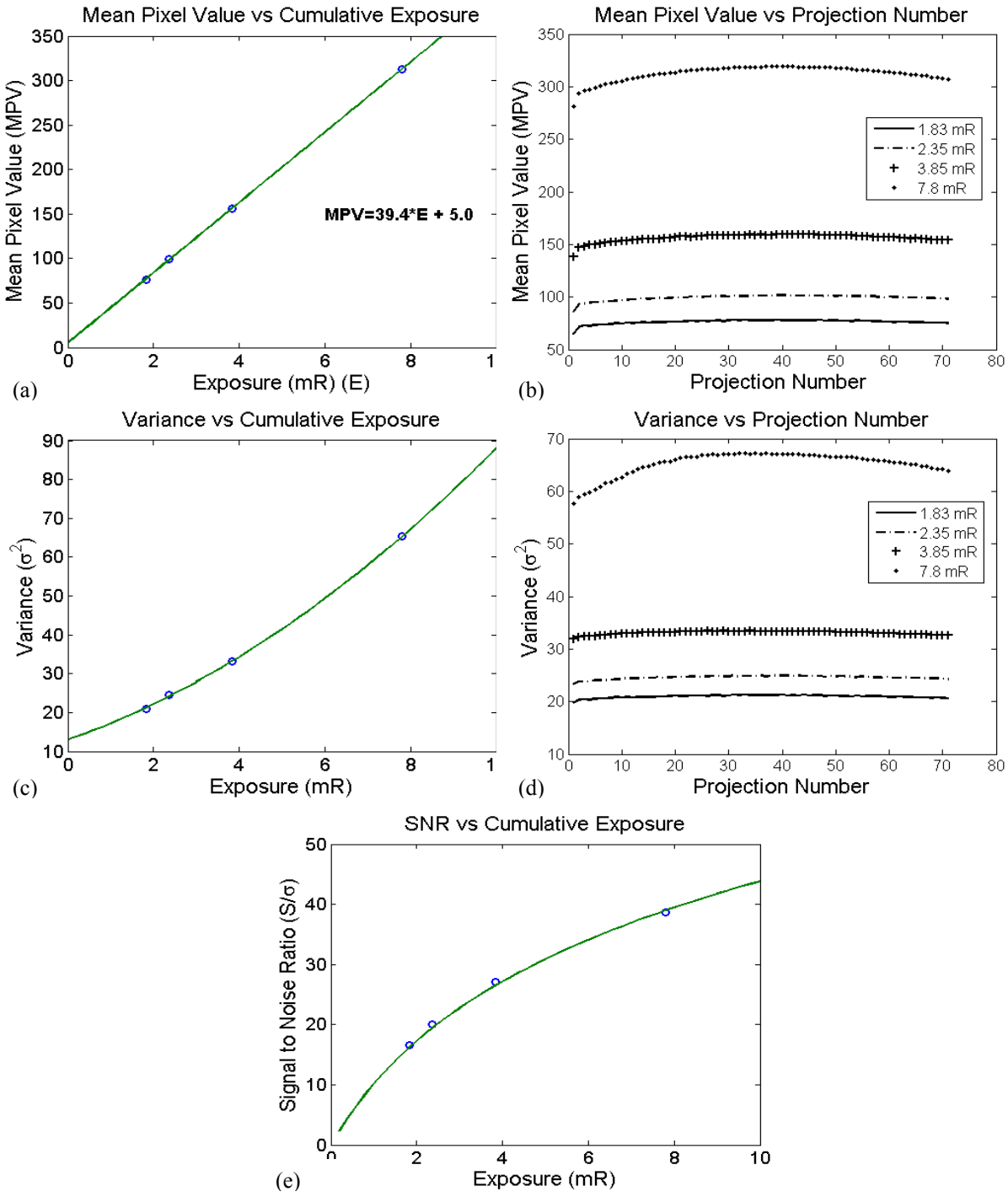

Figure 2: (a) Response of acquisition system relating mean pixel value (MPV) and exposure. (b) MPV as a function of projection angle. (c) Empirical relationship between variance and exposure. (d). Variance as a function of projection angle. (e) SNR as a function of exposure.

Figure 3: Simulated nodules which are added to the projection image prior to noise simulation and reconstruction

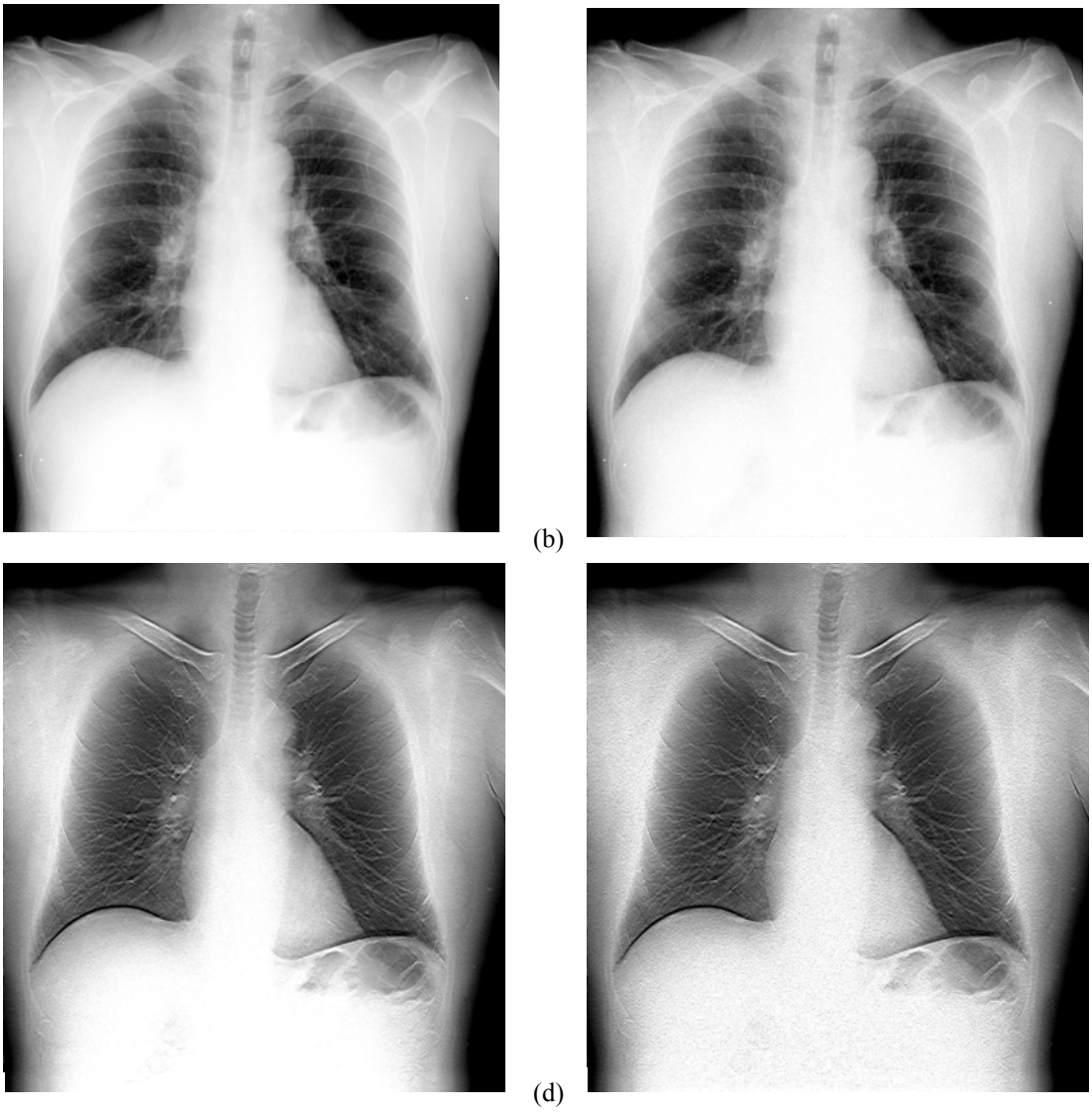

Figure 4: (a) Full dose projection image at 0º. (b) Simulated half dose projection image at 0º. (c) Full dose reconstructed tomosynthesis image (plane14). (d) Simulated half dose reconstructed tomosynthesis image (plane14).

Nodule simulation was performed on each projection image prior to noise simulation. An example of the simulated nodules that were added to the original image is shown in Figure 3.

The resultant projection images, after the noise simulation method was applied, approximate the correct SNR for an image taken at a reduced exposure. This noise propagates through the tomosynthesis reconstruction algorithm and simulates how reduced dose would affect nodule conspicuity and detection accuracy. Figure 4 shows the effect of adding noise to simulate half the exposure of the original image in both the original projections and the resultant tomosynthesis reconstructions.

Figure 5 demonstrates the nodule conspicuity dose response under different conditions. Each ROI shown is 16 cm^2 with the simulated nodule located in the center. The same ROI location was used for each row. The first row shows a 4 mm simulated nodule placed in the lower left lung; the second row shows a 6 mm simulated nodule placed behind a rib; and the third row shows an 8 mm simulated nodule placed in the mediastinum.

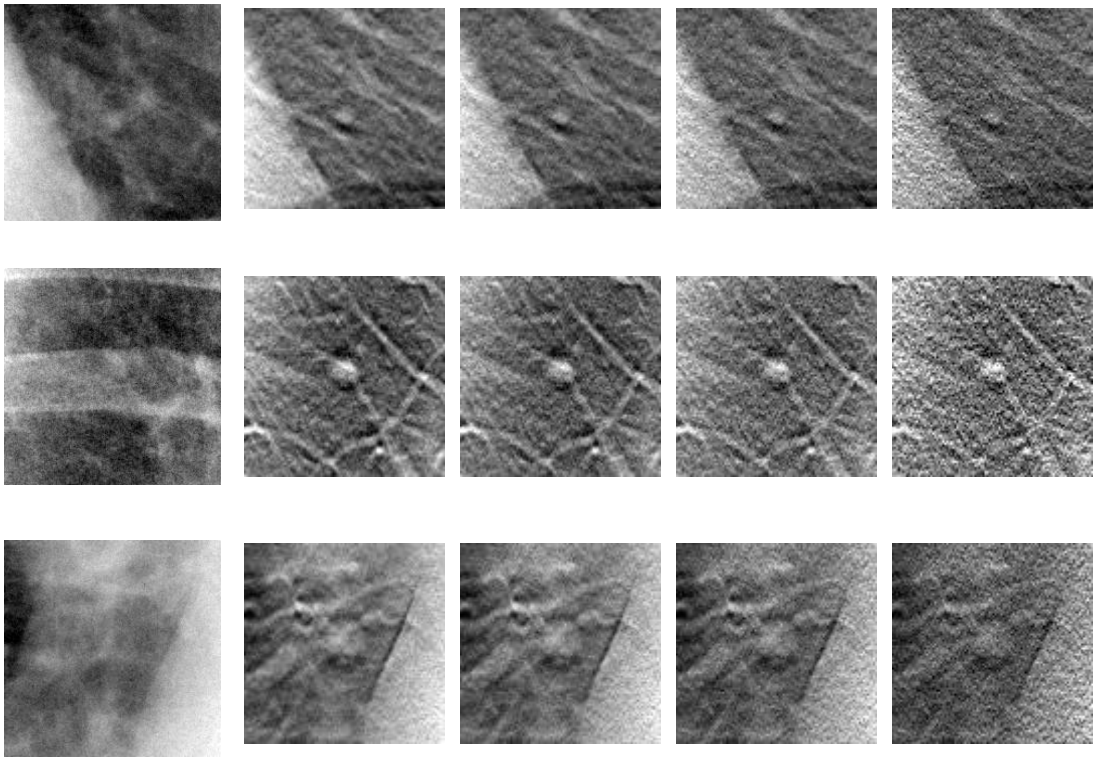

Figure 5: The effect of low dose simulations on nodule consipicuity.
1st column shows the ROI from the projection image at 100% dose;
2nd column is the ROI from the tomosynthesis reconstructed plane at 100% dose;
3rd column is the ROI from the tomosynthesis reconstructed plane at 75% dose;
4th column is the ROI from the tomosynthesis reconstructed plane at 50% dose;
5th column is the ROI from the tomosynthesis reconstructed plane at 25% dose.

Initial subjective analysis of the simulated reduced dose images suggest that this method adequately emulates a tomosynthesis image acquired at a reduced dose. This method will be used in a future study to determine the optimum reduced exposure for tomosynthesis image acquisition.

Discussion
In this study, we made the assumption that the shape of the NNPS would be independent of exposure. There is, nevertheless, some variation due to exposure and an additional step can be implemented which may slightly improve the performance of the method presented in this work. However, with the small amount of variation at these low exposure levels, only a minor improvement can be expected.

Conclusions:
The methodology described, generates tomosynthesis images subjectively equivalent to images acquired at reduced dose. When coupled with simulated nodules, this approach may be used with human observers to conduct ROC studies of observer performance for nodules in both obscured and un-obscured lung.

Future Work:
Clinical subject data with simulated noise and nodules will be used in an ROC study with chest radiologists in order to more accurately determine the detection accuracy in tomosynthesis images at reduced dose levels for dose optimization.

Acknowledgments:
The authors would like to thank Rob Saunders, PhD, and Nicole Ranger, MSc of Duke University for their helpful contributions. This work has been supported in part by NIH (R01 CA80490), DOD W81XWH-06-1-0732, and through a research agreement with GE Healthcare.

This work has not been submitted for presentation or publication elsewhere.

References

[1] J. T. Dobbins, III and D. J. Godfrey, "Digital x-ray tomosynthesis: current state of the art and clinical potential," Physics in Medicine and Biology **48**, R65-R106 (2003).

[2] H. P. McAdams, D. J. Godfrey and J. T. Dobbins, III, "Digital tomosynthesis for improved lung nodule detection: initial clinical experience," RSNA 89th Scientific Assembly (2003).

[3] D. P. Frush, C. C. Slack, C. L. Hollingsworth, et al., "Computer-Simulated Radiation Dose Reduction for Abdominal Multidetector CT of Pediatric Patients," American Journal of Roentgenology **179**, 1107-1113 (2002).

[4] M. Volk, O. W. Hamer, S. Feuerbach and M. Strotzer, "Dose reduction in skeletal and chest radiography using a large-area flat-panel detector based on amorphous silicon and thallium-doped cesium iodide: technical background, basic image quality parameters, and review of the literature," European Radiology **14**, 827-834 (2004).

[5] A. J. Britten, M. Crotty, H. Kiremidjian, A. Grundy and E. J. Adam, "The addition of computer simulated noise to investigate radiation dose and image quality in images with spatial correlation of statistical noise: an example application to X-ray CT of the brain," The British Journal of Radiology **77**, 323-328 (2004).

[6] J. R. Mayo, K. P. Whittall, A. N. Leung, et al., "Simulated Dose Reduction in Conventional Chest CT: Validation Study," Radiology **202**, 453-457 (1997).

[7] M. Bath, M. Hakansson, A. Tingberg and L. G. Mansson, "Method of Simulating Dose Reduction for Digital Radiographic Systems," Radiation Protection Dosimetry **114**, 253-259 (2005).

[8] R. S. Saunders and E. Samei, "A method for modifying the image quality parameters of digital radiographic images," Medical Physics **30**, 3006-3017 (2003).

[9] International Electrotechnical Commission, *Medical diagnostic X-ray equipment - Radiation conditions for use in the determination of characteristics*, (Geneva, Switzerland, 2005).

[10] R. S. Saunders, E. Samei, J. L. Jesneck and J. Y. Lo, "Physical characterization of a prototype selenium-based full-field digital mammography detector," Medical Physics **32**, 588-599 (2005).

[11] J. T. Dobbins, III, E. Samei, N. T. Ranger and Y. Chen, "Intercomparison of methods for image quality characterization. II. Noise power spectrum," Medical Physics **33**, 1466-1475 (2006).

[12] E. Samei, M. J. Flynn and W. R. Eyler, "Detection of Subtle Lung Nodules: Relative Influence of Quantum and Anatomical Noise on Chest Radiographs," Radiology **213**, 727-734 (1999).

[13] R. S. Saunders, E. Samei and C. Hoeschen, "Impact of Resolution and Noise Characteristics of Digital Radiographic Systems on the Detectability of Lung Nodules," SPIE Medical Imaging 2003: Image Processing **Proc. SPIE (in press)**, (2003).

[14] D. J. Godfrey, A. Rader and J. T. Dobbins, III, "Practical strategies for the clinical implementation of matrix inversion tomosynthesis (MITS)," Medical Imaging 2003: Physics of Medical Imaging Conference **Proceedings of SPIE 5030**, 379-390 (2003).

[15] D. J. Godfrey, R. J. Warp and J. T. Dobbins, III, "Optimization of Matrix Inverse Tomosynthesis," Proceedings of SPIE **4320**, 696-704 (2001).

[16] J. T. Dobbins, III, "Matrix Inversion Tomosynthesis improvements in longitudinal x-ray slice imaging (patent)," Journal (1990).